

Long range p -wave proximity effect into a disordered metal

Aydin Cem Kecer,¹ Valentin Stanev,¹ and Victor Galitski^{2,3}

¹*Condensed Matter Theory Center, Department of Physics,
University of Maryland, College Park, MD 20742-4111, USA*

²*Joint Quantum Institute and Condensed Matter Theory Center,
Department of Physics, University of Maryland, College Park, MD 20742-4111, USA*

³*School of Physics, Monash University, Melbourne, Victoria 3800, Australia*

(Dated: August 20, 2014)

We use quasiclassical methods of superconductivity to study the superconducting proximity effect from a topological p -wave superconductor into a disordered one-dimensional metallic wire. We demonstrate that the corresponding Eilenberger equations with disorder reduce to a closed non-linear equation for the superconducting component of the matrix Green's function. Remarkably, this equation is formally equivalent to a classical mechanical system (i.e., Newton's equations), with the Green function corresponding to a coordinate of a fictitious particle and the coordinate along the wire corresponding to time. This mapping allows to obtain exact solutions in the disordered nanowire in terms of elliptic functions. A surprising result that comes out of this solution is that the p -wave superconductivity proximity-induced into the disordered metal remains long-range, decaying as slowly as the conventional s -wave superconductivity. It is also shown that impurity scattering leads to the appearance of a zero-energy peak.

Introduction. – Superconducting heterostructures have attracted a lot of attention recently as possible hosts of Majorana fermions [1–9]. One of the important outstanding questions in the studies of these heterostructures is the interplay between topological superconductivity and disorder [10–13]. Here we explore this issue focusing on the leakage of p -wave superconductivity into a disordered metal. Naïvely, it may not appear to be a particularly meaningful question, because unconventional superconductivity is known to be suppressed by disorder per Anderson's theorem [14]. However, Anderson's theorem is only relevant to an intrinsic superconductor and has little to do with a leakage of superconductivity.

The linearized Usadel equations are standard tools in studies of proximity effects [15, 16]. Their derivation, however, assumes that an anisotropic component of the superconducting condensate's wave-function is small compared to the isotropic one, which is not the case in the systems we are interested in. Here, we focus on the more general Eilenberger equations [17, 18], which allow us to straightforwardly model systems with complicated geometries, and varying degree of disorder. (In the context of topological superconductivity, similar approach has been used in Refs. [19–22].) We obtain exact solutions of these equations, and study superconducting correlations induced by proximity in a metallic wire. In particular, we demonstrate that the p -wave correlations can be surprisingly long-ranged, even in the presence of disorder. We also show that impurity scattering produces a zero-energy peak in the density of states (DOS).

Solution for s -wave and p -wave order parameters. – We study the quasiclassical Green's function \hat{g} , which is a matrix in both Nambu and spin space [18]. It is obtained from the full microscopic Green's function by integrating over the energies close to the Fermi surface, and it faithfully

captures the long lengthscale features of the system [23]. In one-dimensional systems, \hat{g} depends on the Matsubara frequency (ω), the center-of-mass coordinate of the pair (x), and the direction of the momentum at the Fermi points ($\zeta = \mathbf{p}_x/p_F = +1/-1$ for right/left going particles). The Green's function obeys the Eilenberger equation [16–18]

$$\zeta v_F \partial_x \hat{g} = -[\omega \tau_3, \hat{g}] + i[\hat{\Delta}, \hat{g}] - \frac{1}{2\tau_{imp}}[\langle \hat{g} \rangle, \hat{g}]. \quad (1)$$

The effect of impurities enters the equation through the mean time between collisions τ_{imp} , and $\langle \dots \rangle$ denotes an average over the Fermi surface. We ignore self-consistency, and assume that the order parameter $\hat{\Delta}$ is constant throughout the wire. (We believe enforcing self-consistency would not change our results qualitatively.)

We consider s -wave and p -wave order parameters in parallel, even though the appropriate Eilenberger equations differ significantly. First, we decompose the Green's function in Nambu space using the Pauli matrices τ_i : $\hat{g} = -ig_1\hat{\tau}_1 + g_2\hat{\tau}_2 + g_3\hat{\tau}_3$. The scalar functions g_i have to satisfy the normalization condition $-g_1^2 + g_2^2 + g_3^2 = 1$ (This will be referred to as the norm of \hat{g} , from here on). Note that the DOS of the system can be obtained from the diagonal component g_3 [21].

In the case of an s -wave superconductor, $\hat{\Delta}$ is a spin-singlet and, ignoring the spin indices, it can be written as $\Delta_0 i\tau_2$. The diagonal component g_3 contains the particle-hole correlations. The function g_2 encodes the s -wave pairing, whereas g_1 describes the p -wave, odd-frequency superconducting correlations, induced by boundaries or other inhomogeneities (it disappears in the bulk uniform state [24–26]). In the case of a p -wave wire we consider spinless fermions, and the order parameter can be written as $\zeta \Delta_0 i\tau_2$. The difference from the s -wave case arises

from the fact that now g_2 is p -wave, and g_1 contains the secondary s -wave (odd-frequency) correlations [26–28].

The components of \hat{g} obey three coupled differential equations. These equations, however, differ for the s -wave and the p -wave cases, due to the Fermi surface averaging: in the s -wave case we have $\langle g_1 \rangle = 0$, $\langle g_2 \rangle = g_2$, whereas in the p -wave case $\langle g_1 \rangle = g_1$, $\langle g_2 \rangle = 0$. In both cases $\langle g_3 \rangle = g_3$ applies (particle-hole correlations are s -wave-like). We use an index $j = (1, 2)$ that allows us to write the component equations in a unified way; in the s -wave case we have $j = 1$, and $j = 2$ pertains to the p -wave case. This index will be used for the rest of the paper, unless the state is explicitly indicated with a subscript s or p . For the order parameters we have $\Delta_{(1)} \equiv \Delta_s = \Delta_0$ for s -wave, and $\Delta_{(2)} \equiv \Delta_p = \zeta \Delta_0$ for p -wave. In g_j the subscript denotes the Nambu space components – g_1 and g_2 for s -wave and p -wave cases respectively. With these, and using the Kronecker delta δ_{ij} , we write the Eilenberger equation as:

$$\zeta v_F \partial_x g_1 = -2\omega g_2 + 2\Delta_{(j)} g_3 - \left(\frac{1}{\tau_{imp}} g_2 g_3 \right) \delta_{j2}, \quad (2a)$$

$$\zeta v_F \partial_x g_2 = -2\omega g_1 - \left(\frac{1}{\tau_{imp}} g_1 g_3 \right) \delta_{j1}, \quad (2b)$$

$$\zeta v_F \partial_x g_3 = 2\Delta_{(j)} g_1 - (-1)^j \frac{1}{\tau_{imp}} g_1 g_2. \quad (2c)$$

In the clean case, these equations become linear and are easily solved [21, 24, 25]. Impurities introduce nonlinear coupling, proportional to $1/\tau_{imp}$. Nevertheless, as we will demonstrate, these equations can still be treated analytically.

To be integrable, this system (either for s -wave or p -wave state) should have two constants of integration. The norm of \hat{g} is one of them, and it can be shown that another constant is given by:

$$C_{(j)} = \frac{(-1)^{j-1}}{2\tau_{imp}} g_j^2 + 2\Delta_{(j)} g_2 + 2\omega g_3. \quad (3)$$

This can be seen from equations Eq. (2), by verifying that $\partial_x C_{(j)} = 0$, for both s - and p -wave cases. Using $C_{(j)}$ we can derive from the system (Eqs. 2) a second-order equation for a *single* component. In the s -wave case we proceed by differentiating Eq. 2a. Using $C_s \equiv C_{(1)}$ we obtain the following equation:

$$v_F^2 \partial_x^2 g_1 = 4\alpha_s g_1 - \frac{g_1^3}{2\tau_{imp}^2}, \quad (4)$$

where we have defined $\alpha_s = \Omega^2 + C_s/(4\tau_{imp})$, with $\Omega^2 = \omega^2 + \Delta_0^2$. In the case of a p -wave order parameter we differentiate Eq. 2b, and by using $C_p \equiv C_{(2)}$, and defining $\alpha_p = \Omega^2 + C_p/(4\tau_{imp})$, the resulting equation is:

$$v_F^2 \partial_x^2 g_2 = -2\zeta \Delta_0 C_p + 4\alpha_p g_2 - \frac{3\zeta \Delta_0}{\tau_{imp}} g_2^2 + \frac{g_2^3}{2\tau_{imp}^2}. \quad (5)$$

Either of these equations can now be integrated on its own, without *explicit* reference to the other two components. However, once g_j is determined the other components follow from $C_{(j)}$ and $\partial_x g_j$.

We also consider the case of a normal metallic segment in contact with a superconductor with order parameter Δ_0 (for s -wave) or $\zeta \Delta_0$ (for p -wave). To study the superconducting correlations induced in the normal part we can use the Eilenberger equation with the order parameter in the metal set to zero. The constant of integration becomes $C_{(j)} = (-1)^{j-1} g_j^2 / (2\tau_{imp}) + 2\omega g_3$. To streamline notation we introduce the dimensionless constants $\tilde{C}_{(j)} = C_{(j)} / 2\Delta_0$, $\tilde{\alpha}_{(j)} = \alpha_{(j)} / \Delta_0^2$, and $\beta = 1 / (2\tau_{imp} \Delta_0)$. (Note that in these definitions Δ_0 is introduced only as an energy scale.) With these, we can write, for the g_1 component in a normal segment in contact with s -wave wire, the following equation:

$$\xi_0^2 \partial_x^2 g_1 = 4\tilde{\alpha}_s g_1 - 2\beta^2 g_1^3. \quad (6)$$

In the case of a normal wire in contact with a p -wave superconductor we have equation for g_2 :

$$\xi_0^2 \partial_x^2 g_2 = 4\tilde{\alpha}_p g_2 + 2\beta^2 g_2^3. \quad (7)$$

Notice the difference in the sign between the β^2 terms in the two equations.

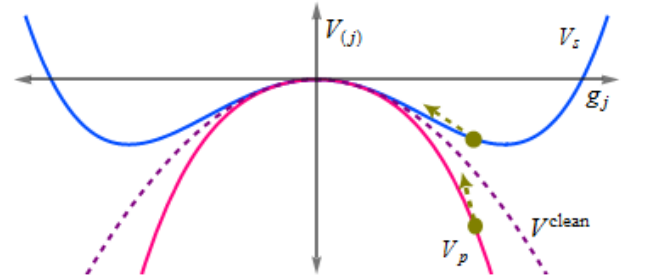


FIG. 1. The potential landscape of a classical particle with motion describing the Green’s function, for a normal metallic segment, in contact with a superconductor. Depending on the superconductor (s or p -wave) potential is either V_s or V_p . In the clean limit both converge to V^{clean} .

Classical particle analogy.– Equations 4, 5, 6 or 7 can be integrated analytically. Before we do this, however, it is instructive to interpret them as equations of motion for a classical particle with one degree of freedom, moving in an external potential. The “position” of this particle is g_j and the “time” t , is given by $\zeta 2x/\xi_0$, hence its “momentum” is $\partial_t g_j$. In both s -wave and p -wave cases the external potential is described by a quartic polynomial function. For example, from Eqs. 6 and 7 we can write $V_{(j)}(g_j) = -\tilde{\alpha}_{(j)} g_j^2 / 2 + (-1)^{j-1} \beta^2 g_j^4 / 8$. Note that V_j describes a double well for the s -wave case ($j = 1$), and a hill for the p -wave case ($j = 2$). In the clean limit we

have $\beta \rightarrow 0$ and the potential energy becomes an inverted parabola, $V_{(j)}(g_j) = -\tilde{\alpha}_{(j)}g_j^2/2$, for both the s -wave and the p -wave cases (see Fig. 1).

We denote the dimensionless “energy” of the classical system by $\tilde{E}_{(j)}$. It is a constant of integration, and can be determined from the boundary conditions for g_j .

Since we want to study proximity effects, we concentrate on Eqs. 6 and 7. After multiplying both sides with $v_F \partial_x g_j$ we integrate the equations two times. The result is the following elliptic integral, where the variable x spans the length of the wire that starts at $x = 0$ and ends at L

$$\int_{g_j(0)}^{g_j(x)} dg_j \left(\tilde{\alpha}_{(j)}g_j^2 + (-1)^j \frac{\beta^2}{4}g_j^4 + 2\tilde{E}_{(j)} \right)^{-1/2} = \pm \frac{2x}{\zeta\xi_0}. \quad (8)$$

The \pm sign before the right hand side of Eq. 8 is to ensure that x is positive, and it depends on the choice of the integration contour in the complex g_j plane. We will denote the poles of the integrand as $\rho_{(j)}^\pm$. The integral can be written in terms of the inverse Jacobi elliptic function sn^{-1} , with elliptic parameter $m = \rho_{(j)}^+/\rho_{(j)}^-$. The monotonic solution is given by

$$\text{sn}^{-1} \left(\frac{g_j(x')}{(\rho_{(j)}^+)^{1/2}} \middle| \frac{\rho_{(j)}^+}{\rho_{(j)}^-} \right) \bigg|_0^x = \pm \frac{\zeta\beta x}{\xi_0} [(-1)^j \rho_{(j)}^-]^{1/2}, \quad (9a)$$

$$\rho_{(j)}^\pm = \frac{2}{\beta^2} \left((-1)^{j-1} \alpha_{(j)} \pm [\alpha_{(j)}^2 - (-1)^j 2\tilde{E}_{(j)}\beta^2]^{1/2} \right). \quad (9b)$$

It is important to note that another choice of the integration contour may lead to non monotonic, and/or oscillatory solutions. We can understand this by considering the classical particle in one of the potentials shown on Fig 1. In the s -wave case, the potential is a double well, hence the motion is generally periodic. However, the non-monotonic solutions are unphysical and we have to discard them, since the turning points of the trajectories scale as $\pm(\omega\tau_{imp})$ at high frequency, and for both $\omega \rightarrow \infty$ or $\tau_{imp} \rightarrow \infty$ the periodic motion has unbounded amplitude. In the p -wave case, the period of the elliptic function is imaginary, as V_p does not lead to periodic motion. We conclude that in both of the s -wave and p -wave cases the only physically acceptable solutions are monotonic (given by Eq. 9). They can be visualized by imagining the motion of a particle, with initial position $g_j(0)$ and velocity directed towards the origin $g_j = 0$, climbing a non-harmonic hill potential $V_{(j)}(g_j)$. The amount of “time”, for the particle to reach its final position represents the length of the wire L . For example, if L is infinite the particle is coming to a stop at the origin (no superconducting correlations at infinity means vanishing velocity), hence should have zero “energy”, $\tilde{E} = 0$.

p-wave wire with normal segment.— Let us use the solution of the Eilenberger equation to study the leakage of

superconductivity in a metallic wire. We consider an infinite wire extending along the x -axis with two segments that meet at $x = 0$. The semi-infinite segment on the left ($x < 0$) is made of clean p -wave superconductor. The segment on the right ($x > 0$) is made of a diffusive normal metal (the order parameter is zero).

We obviously want a solution that, in the limit $x \rightarrow -\infty$ reproduces the mean field result for a uniform clean p -wave superconductor. Introducing the parameter B and the dimensionless variables $\tilde{\Omega} = \Omega/\Delta_0$, $\tilde{\omega} = \omega/\Delta_0$, we can write such a solution [21, 29, 30]:

$$g_1(x) = (1/\tilde{\omega})[1 - \tilde{\Omega}B] \exp(2\tilde{\Omega}x/\xi_0), \quad (10a)$$

$$g_2(x) = \zeta(1/\tilde{\Omega}) \left(1 - [1 - \tilde{\Omega}B] \exp(2\tilde{\Omega}x/\xi_0) \right), \quad (10b)$$

$$g_3(x) = \left\{ [1 - \tilde{\Omega}B]/(\tilde{\Omega}\tilde{\omega}) \right\} \exp(2\tilde{\Omega}x/\xi_0) + \tilde{\omega}/\tilde{\Omega}. \quad (10c)$$

B has to be determined from the boundary conditions at $x = 0$. For simplicity, we will consider the case of perfectly transparent boundary there, which guarantees the continuity of the Green’s functions [31].

Now we consider the diffuse normal segment with infinite length. Then, for $x \rightarrow \infty$ we have $g_1 \rightarrow 0$, $g_2 \rightarrow 0$ and $g_3 \rightarrow \text{sgn}(\omega)$. The constant of integration is $\tilde{C}_p = [-\beta g_2^2/2 + \tilde{\omega}g_3]$, when normalized to $2\Delta_0$. Using the fact that $\tilde{C}_p(0) = \tilde{C}_p(x \rightarrow \infty) = |\tilde{\omega}|$, we immediately obtain $B = (1/\beta)[-1 + (1 + 2\beta[\tilde{\Omega} - |\tilde{\omega}|])^{1/2}]$, with $\tilde{\alpha}_p = \tilde{\omega}^2 + \beta|\tilde{\omega}|$.

We can understand intuitively the behavior of g_2 by again invoking the classical analogy. The particle in potential V_p , with “position” g_2 where time is $\tilde{t} = 2x/\xi_0$, starts at $g_2(0) = \zeta B$, with velocity $\partial_{\tilde{t}}g_2(0) = -\tilde{\omega}\zeta g_1(0) = -\zeta(1 - \tilde{\Omega}B)$, and moves towards its unstable equilibrium point $g_1(+\infty) = 0$, gradually slowing down until $\partial_{\tilde{t}}g_2(+\infty) = 0$. Thus, the trajectory of g_2 satisfies $\tilde{E}_p = 0$. The integral in Eq. 8 is now straightforward, and defining the dimensionless constant $\kappa = [1 + \beta^2 B^2/(4\tilde{\alpha}_p)]^{1/2}$, we can write the solution for g_2 :

$$g_2(x) = \frac{\zeta B}{\cosh(x/\xi') + \kappa \sinh(x/\xi')}. \quad (11)$$

Here $\xi' = \xi_0/(2\tilde{\alpha}_p^{1/2})$ gives the effective decay length of the solution (at $T = 0$). In physical units it is

$$\xi' = \frac{v_F}{\sqrt{4\omega^2 + 2|\Delta_0\omega/(\tau_{imp})|}}. \quad (12)$$

In the dirty limit we have $\xi' = \sqrt{D/|\omega|}$, where D is the diffusion coefficient. Finally, in the clean limit g_2 converges to $\zeta B \exp(-2|\tilde{\omega}|x/\xi_0)$, as expected [21].

The other two components of the Green’s function can be derived from g_2 using \tilde{C}_p and the Eilenberger equations: $g_1 = -\zeta\xi_0\partial_x g_2/(2\tilde{\omega})$ and $g_3 = \text{sgn}(\tilde{\omega}) + \beta g_2^2/(2\tilde{\omega})$. As expected, impurities suppress g_2 relative to g_1 . However, they both decay in the normal segment over the

same lengthscale, given by Eq. 12. This decay is long-range, and furthermore, with exactly the same length-scale we obtain for the case of s -wave order parameter (see below). Thus, the naïve expectation of strong suppression of the p -wave correlations is misleading in this case. This is one of the main points of our paper.

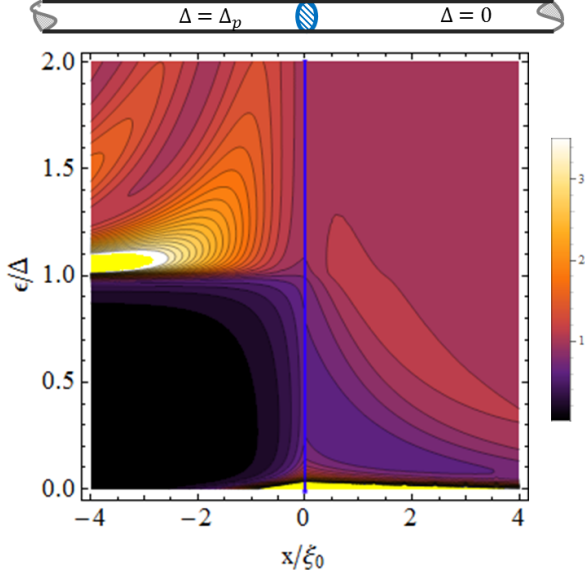


FIG. 2. Contour plot of the DOS of an infinite wire. There is moderate disorder ($\beta = 1$) in the normal segment ($x > 0$). The solid yellow marks the regions that are beyond the plot range (where $N/N_0 > 3.5$). Notice the zero-energy peak in the normal segment.

We can now obtain the DOS of the system, which is proportional to the real part of $g_3(\omega \rightarrow -i\epsilon + \delta)$. On Fig. 2 we show the DOS for a system with moderate amount of disorder. Several things are apparent from this plot. First, for energies below Δ_0 there is a significant decrease in the DOS of the normal segment, caused by the proximity effect; however, it is not a real gap, since the DOS stays finite everywhere. This decrease is entirely due to impurities – in the clean case the DOS is constant for $x > 0$ [21]. The impurity-induced term in g_3 also has a divergence in the limit of small frequencies ($g_3 \sim 1/\omega$), which leads to an infinite peak in the DOS. This zero-energy peak has the same origin as the Majorana edge state (namely, the sign change in the order parameter [29, 30, 33]). Thus, in the infinite wire case, impurity scattering creates zero-energy peak, but it is not sufficient to localize it exponentially.

As a side note, if the p -wave superconductor was replaced by an s -wave superconductor, the solution to Eq.(6) would be $g_1 = \zeta A [\cosh(x/\xi') + \kappa_s \sinh(x/\xi')]^{-1}$. Here, $\kappa_s = [1 - \beta^2 A^2 / (4\tilde{\alpha}_s)]^{1/2}$ and ζA is the value of g_1 at the junction, and is determined by the boundary values at the infinities in a way similar to that in the p -wave case. However, unlike the p -wave case, the g_1 component

at the boundary is proportional to $\tilde{\omega}$. This dependence on $\tilde{\omega}$ changes the zero energy behavior of the DOS as follows. From $g_3 = \text{sgn}(\tilde{\omega}) - \beta/(2\tilde{\omega})g_1^2$, we see that the low frequency limit is finite and thus there is no zero energy peak in the s -wave case [32].

If the normal segment has finite length L , we impose the condition $g_2(L) = 0$, since the p -wave component is suppressed by the reflection from the boundary. Then the solution follows immediately from Eq. 9 as $g_2(x) = \zeta(\rho_p^+)^{1/2} \text{sn}[\beta(\rho_p^-)^{1/2}(x-L)/\xi_0]$, with elliptic parameter $m = \rho_p^+/\rho_p^-$. However, this expression has limited practical value. The unknown constant B_L , which should be obtained from matching the two solutions for g_2 at $x = 0$, enters the expression through the parameters ρ_p^\pm , which makes it difficult to solve. Fortunately, an approximate analytic form for B_L can be obtained. In the limit $L \rightarrow \infty$, B_L converges to B , that was previously calculated for the infinite wire case. In the opposite limit, $L \rightarrow 0$, B_L vanishes. Numerical investigation suggests that B_L as a function of L can be approximated by $B[1 - \exp(-2L/\lambda_B)]$, where the length scale λ_B controls how quickly B_L approaches to the infinite wire limit with increasing L . By expanding the integral in Eq. 8 around $B = 0$ and matching it with the approximate expression, we obtain $\lambda_B = B\xi_0$. Once we have B_L , we can use ad-

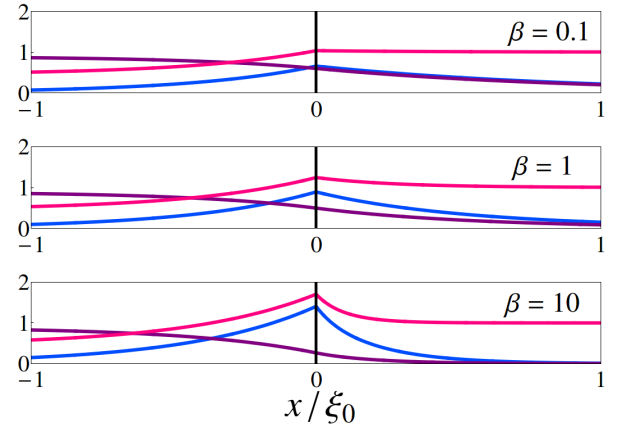


FIG. 3. Components of \hat{g} , (g_1 : blue, g_2 : purple, g_3 : red) for a wire with infinite p -wave section and finite disordered section of length $L = 5\xi_0$. Top panel: weak disorder ($\beta = 1/(2\tau_{imp}\Delta_0) = 0.1$). Middle panel: moderate disorder ($\beta = 1$). And bottom panel: strong disorder ($\beta = 10$). The Matsubara frequency is set to $\omega = \Delta_0/2$.

dition and transformation rules for elliptic functions [34] to write g_2 in a form that manifestly converges to that of the $L = \infty$ case. To save space, we shorten the common argument of elliptic functions, $\beta|\rho_p^-|^{1/2}x/\xi_0$ as (\cdot) . The common elliptic parameter of the elliptic functions is $(\rho_p^- - \rho_p^+)/\rho_p^-$, and it lies in the interval $[0, 1]$. With

these definition we get:

$$g_2(x) = \zeta \frac{B_L \text{dn}(\cdot) - \text{sn}(\cdot) \text{cn}(\cdot) \sqrt{|\rho_p^+| + B_L^2} \sqrt{1 + B_L^2/|\rho_p^-|}}{\text{cn}^2(\cdot) - (B_L^2/|\rho_p^-|) \text{sn}^2(\cdot)} \quad (13)$$

We can again obtain the two other components from g_2 by using: $g_1 = -\zeta \xi_0 \partial_x g_2 / (2\tilde{\omega})$ and $g_3 = (\tilde{\alpha}_p - \tilde{\omega}^2) / (\beta \tilde{\omega}) + \beta g_2^2 / (2\tilde{\omega})$.

As $L \rightarrow \infty$, \tilde{E}_p tends to zero, the elliptic functions are replaced by their hyperbolic counterparts, and we recover the solution for the infinite wire case (Eq. 11).

Again, it is the impurity-induced contribution to g_3 that is of most interest. After analytic continuation we can write the zero-energy limit as:

$$g_3(x) = \frac{1}{\pi} \delta(\epsilon) \mathcal{M}(x). \quad (14)$$

The function $\mathcal{M}(x)$ describes the x -dependent weight of the zero energy mode, and we can extract it from Eq. 13. Its values at the junction point and at the end of the wire are $\mathcal{M}(0) = 1 - B_L$ and $\mathcal{M}(L) = \mathcal{M}(0) - \beta B_L^2 / 2$ respectively. It can be approximated by a decaying exponent with decay length $\lambda_M = \xi_0 \beta B_L / (4\tilde{\alpha}_p + 2\beta^2 B_L^2)$. Thus, in sharp contrast with the $L = \infty$ case, the zero-energy peak of a finite wire is exponentially localized. Figure 4 shows $\mathcal{M}(x)$ in the normal section with length $L = 5\xi_0$, for various disorder strengths. As can be seen, $\mathcal{M}(x)$ (i.e., the zero-energy peak) becomes more localized as the disorder in the normal section increases.

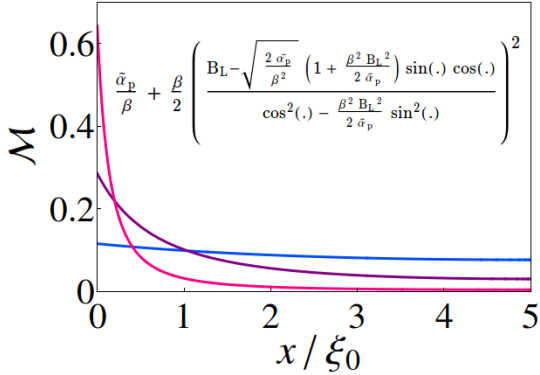


FIG. 4. The weight of the zero energy mode $\mathcal{M}(x)$ in a normal section with length $L = 5\xi_0$ for three disorder strengths (blue: $\beta = 1/(2\tau_{imp}\Delta_0) = 0.1$, purple: $\beta = 1$, red: $\beta = 10$). The expression in the inset is deduced from (13), and (\cdot) stands for $(2\tilde{\alpha}_p)^{1/2}x/\xi_0$.

This research was supported by DOE-BES DESC0001911 (VG & VS), NSF-CAREER DMR-0847224 (ACK), and Simons Foundation.

- [1] L. Fu and C.L. Kane, Phys. Rev. Lett. **100**, 096407 (2008).
- [2] J. D. Sau, R. M. Lutchyn, S. Tewari, and S. Das Sarma, Phys. Rev. Lett. **104**, 040502 (2010).
- [3] J. Alicea, Phys. Rev. B **81**, 125318 (2010).
- [4] R.M. Lutchyn, J.D. Sau, and S. Das Sarma, Phys. Rev. Lett. **105**, 077001 (2010).
- [5] Y. Oreg, G. Refael, and F. von Oppen, Phys. Rev. Lett. **105**, 177002 (2010).
- [6] M. Wimmer, A. R. Akhmerov, M. V. Medvedyeva, J. Tworzydo, C. W. J. Beenakker, Phys. Rev. Lett. **105**, 046803 (2010).
- [7] V. Mourik, K. Zuo, S. Frolov, S. Plissard, E. Bakkers, and L. Kouwenhoven, Science **336**, 1003 (2012).
- [8] M.T. Deng, C.L. Yu, G.Y. Huang, M. Larsson, P. Caroff, and H.Q. Xu, Nano Lett. **12**, 6414 (2012).
- [9] A. Das, Y. Ronen, Y. Most, Y. Oreg, M. Heiblum, and H. Shtrikman, Nat. Phys. **8**, 887 (2012).
- [10] P.W. Brouwer, M. Duckheim, A. Romito, and F. von Oppen, Phys. Rev. B **84**, 144526 (2011).
- [11] A. R. Akhmerov, J. P. Dahlhaus, F. Hassler, M. Wimmer, and C. W. J. Beenakker, Phys. Rev. Lett. **106**, 057001 (2011).
- [12] W. DeGottardi, D. Sen, and S. Vishveshwara, New J. Phys. **13**, 065028 (2011).
- [13] A. M. Lobos, R. M. Lutchyn, and S. Das Sarma, Phys. Rev. Lett. **109**, 146403 (2012).
- [14] P. W. Anderson, J. Phys. Chem. Solids **11**, 26 (1959).
- [15] K. L. Usadel, Phys. Rev. Lett. **25**, 507 (1970).
- [16] F. S. Bergeret, A. F. Volkov, and K. B. Efetov, Rev. Mod. Phys. **77**, 1321 (2005), and references therein.
- [17] G. Eilenberger, Z. Phys. **214**, 195 (1968).
- [18] See, for example, N. B. Kopnin, "Theory of Nonequilibrium Superconductivity" (Clarendon Press, Oxford) 2001.
- [19] P. Neven, D. Bagrets, and A. Altland, New J. Phys. **15**, 055019 (2013).
- [20] S. Abay, D. Persson, H. Nilsson, F. Wu, H.Q. Xu, M. Fogelström, V. Shumeiko, and P. Delsing, Phys. Rev. B **89**, 214508 (2014).
- [21] V. Stanev, and V. Galitski, Phys. Rev. B **89**, 174521 (2014).
- [22] H.-Y. Hui, J. D. Sau, and S. Das Sarma, arXiv:1406.4853.
- [23] For a recent comparison between quasiclassical and fully microscopic calculation of the same structure, see, for example, C. Reeg, and D. Maslov, Phys. Rev. B **90**, 024502 (2014).
- [24] F.S.Bergeret, A.F. Volkov, K.B.Efetov, Phys. Rev. B **65**, 134505 (2002).
- [25] I. Baladié and A. Buzdin, Phys. Rev. B **64**, 224514 (2001).
- [26] A. Golubov, Y. Tanaka, Y. Asano, and Y. Tanuma, J. Phys.: Condens. Matter **21**, 164208 (2009)
- [27] Y. Tanaka, M. Sato, and N. Nagaosa, J. Phys. Soc. Jpn. **81**, 011013 (2012), and references therein.
- [28] Note that the odd-frequency correlations are different from the odd-frequency order parameter, which was originally proposed for ^3He by Berezinskii (V. L. Berezinskii, JETP Lett. **20**, 287 (1975)), and was later studied in the context of curpates (A. Balatsky, and E. Abrahams, Phys. Rev. B **45**, 13125 (1992), A. Balatsky, E. Abra-

- hams, D. J. Scalapino, and J. R. Schrieffer, Phys. Rev. B **52**, 1271 (1995)).
- [29] M. Matsumoto and M. Sigrist, J. Phys. Soc. Jpn. **68**, 994 (1999).
- [30] M. Matsumoto, M. Koga, and H. Kusunose, J. Phys. Soc. Jpn. **82**, 034708 (2013).
- [31] More realistic modeling of the boundary requires more complicated boundary conditions: A. V. Zaitsev, Zh. Eksp. Teor. Fiz. 86, 1742 (1983) [Sov. Phys. JETP **59**, 1015 (1984)], and G. Kieselmann, Phys. Rev. B **35**, 6762 (1987).
- [32] Analogous calculation in the s -wave case leads not to a peak, but linear suppression of DOS at low energies. The overall DOS profiles are very similar to those obtained earlier numerically (see, e.g., W. Belzig, C. Bruder, and G. Schon, Phys. Rev. B, **54**, 9443 (1996)).
- [33] See also A. Fauchre, W. Belzig, and G. Blatter, Phys. Rev. Lett. **82**, 3336 (1999).
- [34] I. S. Gradshteyn, I. M. Ryzhik, *Table of integrals, tables and products*, Alan Jeffrey and Daniel Zwillinger (eds.) Seventh edition (Academic 2007), Section 8.1